Molecular Human Reproduction, Vol.15, No.2 pp. 89–103, 2009
Advanced Access publication on January 13, 2009 doi:10.1093/molehr/gan082

MHR Basic science of reproductive medicine

ORIGINAL RESEARCH

Gene expression microarray profiles of cumulus cells in lean and overweight-obese polycystic ovary syndrome patients

Shlomit Kenigsberg[1,†] Yaakov Bentov[2,†,‡], Vered Chalifa-Caspi[3], Gad Potashnik[2], Rivka Ofir[1], and Ohad S. Birk[1,4,5]

[1]The Morris Kahn Laboratory of Human Genetics, National Institute for Biotechnology in the Negev, Ben-Gurion University, Beer-Sheva 84105, Israel [2]Fertility and IVF Unit, Soroka University Medical Center, Beer-Sheva 84101, Israel [3]Bioinformatics Core Facility at the National Institute for Biotechnology in the Negev (NIBN), Ben-Gurion University, Beer-Sheva 84105, Israel [4]Genetics Institute at Soroka University Medical Center, Faculty of Health Sciences, Ben-Gurion University, PO Box 151, Beer-Sheva 84105, Israel

[5]Corresponding author: Tel: +972 8-6403439; Fax: +972 8-6400042; Email: obirk@bgu.ac.il

ABSTRACT: The aim of this work was to study gene expression patterns of cultured cumulus cells from lean and overweight-obese polycystic ovary syndrome (PCOS) patients using genome-wide oligonucleotide microarray. The study included 25 patients undergoing *in vitro* fertilization and intra-cytoplasmic sperm injection: 12 diagnosed with PCOS and 13 matching controls. Each of the groups was subdivided into lean (body mass index (BMI) < 24) and overweight (BMI > 27) subgroups. The following comparisons of gene expression data were made: lean PCOS versus lean controls, lean PCOS versus overweight PCOS, all PCOS versus all controls, overweight PCOS versus overweight controls, overweight controls versus lean controls and all overweight versus all lean. The largest number of differentially expressed genes (DEGs), with fold change (FC) $|FC| \geqslant 1.5$ and *P*-value < 0.01, was found in the lean PCOS versus lean controls comparison (487) with most of these genes being down-regulated in PCOS. The second largest group of DEGs originated from the comparison of lean PCOS versus overweight PCOS (305). The other comparisons resulted in a much smaller number of DEGs (174, 109, 125 and 12, respectively). In the comparison of lean PCOS with lean controls, most DEGs were transcription factors and components of the extracellular matrix and two pathways, Wnt/β-catenin and mitogen-activated protein kinase. When comparing overweight PCOS with overweight controls, most DEGs were of pathways related to insulin signaling, metabolism and energy production. The finding of unique gene expression patterns in cumulus cells from the two PCOS subtypes is in agreement with other studies that have found the two to be separate entities with potentially different pathophysiologies.

Key words: PCOS / cumulus / microarray / infertility / insulin resistance

Introduction

Polycystic ovary syndrome (PCOS) is a common heterogeneous endocrinopathy in women of reproductive age, which is mostly associated with ovulation failure. The PCOS phenotype is variable and may include polycystic ovaries, hirsutism, hyperandrogenism and pre-diabetes (Franks, 1995). The phenotype of PCOS and its impact on reproductive function are profoundly affected by obesity which, in turn, has both genetic and environmental influences (Salehi *et al.*, 2004). PCOS is considered by some authors to be a unique representation of the metabolic syndrome (Sam and Dunaif, 2003).

The etiology of PCOS remains unclear (Diamanti-Kandarakis and Piperi, 2005; Vink *et al.*, 2006); however, the observation of familial segregation of PCOS is consistent with a genetic basis for this disorder. Studies in sisters have shown that hyperandrogenism is the component with the strongest concordance (Legro *et al.*, 1998; Franks *et al.*, 2006). More than 50 candidate genes have been studied for association with the syndrome, but none have been proven to play a definitive role (Escobar-Morreale *et al.*, 2005). Association and linkage studies have provided evidence for linkage disequilibrium at D19S884, a dinucleotide-repeat marker, closely linked to the insulin receptor gene locus on chromosome 19p13.2

†The first two authors contributed equally to the study.

‡Recipient of the American Physician Fellowship for Medicine in Israel.

(Stewart et al., 2006). It has been suggested that X-linked genes and chromosome X inactivation are involved in the determination of the distribution and presentation of the syndrome (Hickey et al., 2006).

Studies comparing gene expression arrays in tissues of PCOS and control patients have reported similar pathways for differentially expressed genes (DEGs) in theca cells (Wood et al., 2004), whole ovaries (Jansen et al., 2004; Oksjoki et al., 2005) and oocytes (Wood et al., 2007). Comparative analysis revealed genes involved in the Wnt/β-catenin and mitogen-activated protein kinase (MAPK)-signaling pathways, retinoic acid metabolism and apoptosis. However, to the best of our knowledge, gene expression in cumulus cells isolated from PCOS patients has never been studied.

The cumulus cells are a subset of granulosa cells which maintain an intimate connection with the oocyte and are responsible for providing several trophic and metabolic factors to the pre-ovulatory oocyte. Both cumulus and granulosa cells are the major source of estradiol. High levels of estradiol prevent the rise of follicle-stimulating hormone (FSH), an essential factor for follicular growth and ovulation induction, which in turn leads to anovulation, a major feature of PCOS. Indeed, the first line of treatment for PCOS, Clomiphen citrate or Letrozole, acts by reducing the effect of estrogen in order to treat anovulation (Speroff and Fritz, 2005).

Cultured luteinized granulosa cells from PCOS have been shown to maintain their unique functional qualities, despite being separated from the rest of the follicular structures, for as long as 12 days (Agrawal et al., 2002). However, unlike the granulosa cells which need to be isolated from the follicular fluid and might include theca cells and lymphocytes, cumulus cells are well-defined, homogeneous cells (Quinn et al., 2006). Therefore, in the current study, we used cultured cumulus cells isolated from patients undergoing *in vitro* fertilization (IVF) in order to minimize the effect of the hormonal stimulation. The patients, divided into PCOS and control groups, were further subdivided into four subgroups: lean PCOS, overweight-obese PCOS, lean controls and overweight-obese controls. We hypothesized that comparisons of gene expression in cumulus cells from PCOS patients versus controls, and between the lean PCOS and obese PCOS subgroups, would elucidate distinct gene expression patterns, allowing insights to molecular mechanisms of PCOS.

Materials and Methods

Patient selection and tissue collection

This study was approved by the Institutional Ethical Review Board of Soroka Medical Center and the committee for genetic experiments of the Israeli Ministry of Health. All the patients signed an informed consent form. Twenty-five patients were enrolled in the study (Table I): 13 PCOS patients—6 lean (LP) with body mass index (BMI) 19–24 and 7 overweight (OP) with BMI 27–34; 12 non-PCOS controls—6 lean (LN) with BMI 19–24 and 6 overweight (ON) with BMI 27–34. After quality assurance, two arrays were excluded from the analysis, one from the ON group and the other from the LP group. The average age of the patients was 31 years (range 29–32). The lean PCOS had a higher ratio of LH/FSH.

All the participants included in the study were women undergoing *in-vitro* fertilization with intra-cytoplasmic sperm injection (IVF–ICSI) at the Soroka Medical Center IVF unit. All the IVF–ICSI cycles included in the study were conducted according to the long mid-luteal GnRH agonist (Diphereline 3.75 mg, PharmaBiotech, Paris, France) protocol. Controlled ovarian stimulation was conducted with recombinant FSH (Follitropin Alfa, Serono, London, UK). The indication for ICSI treatment was combined male factor, poor fertilization rate on standard IVF or as routine for the first IVF cycle on half of the oocytes. Oocyte injections and embryo cultures were performed as described elsewhere (Geary and Moon, 2006). PCOS patients were diagnosed according to the Rotterdam revised criteria after ruling out secondary causes.

Cumulus cell preparation and culture

Following oocyte retrieval, cumulus cells were mechanically stripped from the oocyte after brief exposure to 80 IU/ml hyaluronidase (Cook, Brisbane, Australia) in preparation for the ICSI procedure, by aspiration through a glass pipette with ~200 μm inner diameter (Geary and Moon, 2006). To reduce the effect of gonadotrophin on the cumulus cells, cells were cultured for 48 h in the original IVF plate, as described previously for granulosa cells (Rice et al., 2005). Briefly, the cumulus cells were washed three times with Dulbecco's modified Eagle's medium/Ham's F12 (1:1,) supplemented with penicillin, streptomycin and amphotericin, and resuspended in the same medium supplemented with 10% fetal calf serum. Cells were incubated for 48 h at 37°C with 5% CO_2. Medium was replaced after 24 h.

RNA isolation

Total RNA was extracted using TRI-Reagent (MRC, Cincinnati, OH, USA) to obtain ~2 μg of RNA, which was eluted in a final volume of 20 μl. Concentration and quality were assessed using NanoDrop ND-100 spectrophotometer (NanoDrop Technologies Inc., Wilmington, Delaware, USA). RNA was stored at −80°C until further analysis.

Microarray hybridization

RNA samples were further processed at the DNA microarray laboratory core facility, using the 'Small Sample Target Labeling Assay v.2' protocol from Affymetrix (Santa Clara, CA, USA). Briefly, biotin-labeled cRNA prepared from 50 ng RNA from each patient was fragmented and hybridized to individual U133 + 2.0 arrays using the GeneChip Fluidics Station 400 protocol, and scanned using the Agilent GeneArray Scanner (Affymetrix). Overall, 25 microarray chips were analyzed in this study.

Table I Details of the subgroups of patients

Group name	Group symbol	Number of patients	BMI	LH/FSH ratio
Lean PCOS	LP	5	22 ± 3	1.0–2.6
Lean non-PCOS controls	LN	6	20 ± 4	0.4–1
Overweight-obese PCOS	OP	7	32 ± 4.5	0.4–1.8
Overweight-obese non-PCOS controls	NP	7	31 ± 4.5	0.3–1.1

Gene expression analysis

Raw CEL microarray files were read into the Affy package of affyImGUI, a graphical user interface for the analysis of Affymetrix microarray data using the Linear Modes for MicroArray data (Limma) package (Smyth, 2004). Background adjustment, quantile normalization and probe summarization were achieved by robust multiarray averaging (Irizarry *et al.*, 2003). Quality assessment was performed using R, SpotFire DecisionSite and Pertek® through distribution and box plots, scatter plots, principal component analysis and hierarchical clustering of the samples. A linear model was fitted to the expression data (the log-intensity values) for each gene. Empirical Bayes and other shrinkage methods were used to borrow information across genes, making the analyses stable even for experiments with small number of arrays. Batch information was treated using the block parameter in Limma's 'lmfit' function, with a fixed value of 0.06 for the correlation. Six binary comparisons were computed in Limma: (i) lean comparison: PCOS versus non-PCOS samples (LP/LN), (ii) overweight comparison: PCOS versus non-PCOS samples (OP/ON), (iii) disease comparison: PCOS versus non-PCOS samples (PS/NP), (iv) PCOS comparison: overweight-obese versus lean (OP/LP), (v) controls comparisons: overweight-obese non-PCOS versus lean non-PCOS (ON/LN) and (vi) weight comparison: overweight-obese versus lean (O/L). The probe sets which had a *P*-value <0.01 and fold change in linear scale $\geqslant|1.5|$ in at least one of the comparisons were considered as DEGs. The data were deposited in NCBI's Gene Expression Omnibus (GEO) and are accessible through GEO Series accession number GSE10946 (http://www.ncbi.nlm.nih.gov/geo/).

The Venn diagram was constructed using the Venny tool (Oliveros, 2007) and contains the four main comparison groups. Only probe sets with log2 signal intensity >5 in at least one array, and $P<0.01$ and fold change $|FC|\geqslant 1.5$ in at least one of the comparisons, were included.

Hierarchical clustering of the genes was conducted with SpotFire, using Pearson's correlation and complete linkage.

Gene annotation

Gene annotations were performed using the Netaffx server (www.affymetrix.com), and the Ovarian Kaleidoscope Database (http://ovary.stanford.edu) in order to find a potential role in ovarian physiology and pathogenesis of the disease.

Quantitative polymerase chain reaction (qPCR) validation

For validation of DEGs, 200 ng of RNA were reverse-transcribed into first-strand cDNA using the Reverse-iT 1st Strand Synthesis Kit (ABgene, Epsom, UK) in final volume of 20 μl. Duplicate samples of pooled cDNA from three patients were used for the PCR. Gene-specific primers were designed for the corresponding sequence of probe sets (see list of primers in Table II). The reaction was carried out using Absolute QPCR SYBR green (ABgene) in a final volume of 15 μl on the Corbett Rotorgene 3000 (Corbett Life Science, Australia). Cycling conditions were: 94°C for 15 min, followed by 35 cycles of 94°C for 30 s, 65°C for 15 s and 72°C for 30 s, and a final melting step (78–99°C). The fluorescence crossing threshold (Ct) value was calculated with Rotorgene 3000 system software. The calculation of relative change in mRNA was performed with the efficiency delta-delta Ct method (Pfaffl, 2001), with normalization for the housekeeping gene GAPDH as described elsewhere (Fleige *et al.*, 2006).

Results

Cumulus cells from each of the participants were cultured for 48 h under the same conditions, followed by RNA extraction. RNA from each of the participants was analyzed on a separate microarray chip. Six comparisons were made: lean PCOS versus lean controls (LP/LN), overweight PCOS versus overweight controls (OP/ON), all PCOS versus all controls (PS/NP), overweight PCOS versus lean PCOS (OP/LP), overweight non-PCOS versus lean non-PCOS (ON/LN) and overweight versus lean (O/L).The Venn diagram (Fig 1) describes the number of DEGs with a *P*-value <0.01 and $|FC|\geqslant 1.5$ found with each of the comparisons. The numbers in the overlapping parts of the circles represent the number of genes that were differentially expressed in respective comparisons. Tables A1 (Appendix) contain the probe sets that were differentially expressed in each of the comparisons, the genes they represent, their relative FC, *P*-value and annotation. Due to the length of the gene list, only genes with a fold change greater than two are shown. The full list of DEGs is available upon request.

The LP/LN comparison included 487 probe sets, 78% (375/487) of which showed decreased expression in lean PCOS cumulus cells. Note that 96% of the genes that were annotated as transcription factors were down-regulated in PCOS (44/46). The most prominent pathways in this group were the Wnt/β-catenin and MAPK-signaling pathways, with 27 related genes. These included genes such as *TCF7L2*, *DACT1* and *WNT5a*. Interestingly, a group of genes encoding extracellular matrix constituents and proteins of the innate immune system showed increased expression in the LP cells.

The OP/ON comparison yielded 174 DEGs with 60% of them (105/174) demonstrating decreased expression in the overweight PCOS group. Up-regulation of genes associated with various insulin-signaling pathways, diabetes and obesity was observed, including the insulin receptor (INSR), the leptin receptor (LEPR) and genes participating in the Dentatorubropallidoluysian atrophy (DRPLA) pathway, which mediates insulin's effect on cells (Okamura-Oho *et al.*, 1999).

The comparison of all PCOS with all non-PCOS (PS/NP), disregarding the BMI criterion, yielded only 109 probe sets, 55% of which (60/109) demonstrated decreased expression in the PCOS group. The comparison of obese with lean PCOS samples (OP/LP) revealed 305 DEG probe sets, 68% of which (206/305) demonstrated increased expression in the overweight PCOS group compared with the lean PCOS group.

Eighty-five of the DEGs overlapped in the LP/LN and LP/OP comparisons, representing 17 (85/487) and 28% (85/305) of the genes,

Table II qPCR primers

Gene name	Primers
MRO-F	GAAAGGTTTGGGTTCCTTCTTCAT
MRO-R	TGGAGAACAGGCTTGAAATGTTGT
HAPLN1-F	TCACACAGAGGTGGCAATGT
HAPLN1-R	TGCCTCCCTTCAGAAACACT
CALR-F	TGGAAGACGATTGGGACTTC
CALR-R	CTGAATCACTGGGGGTTCC
OGT-F	CCTGCCCCAGAACCGTATCA
OGT-R	GCAAGTGAGCTGGGATGCTG
FLNA-F	AAAGTCACAGGCCCCCGTCTC
FLNA-R	CCTTGAGCAGGTAGGACACGC

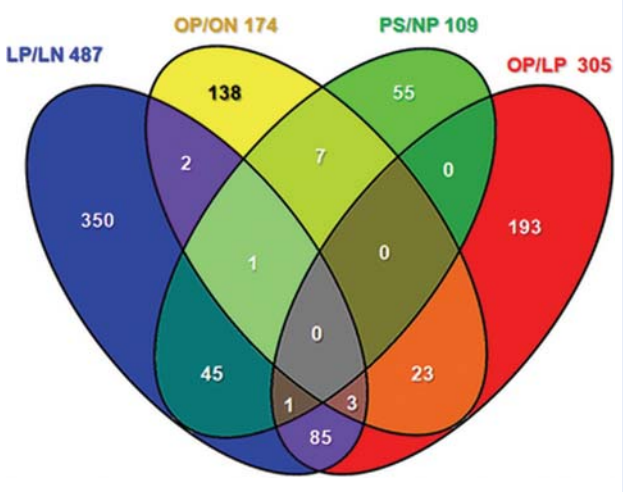

Figure 1 Venn diagram representing the number of DEGs in each comparison and the overlaps between the four main comparison groups. Probe sets with $P < 0.01$ and $|FC| \geqslant 1.5$ in at least one of the comparisons are included.

respectively. Only six genes overlapped between the lean comparison (LP/LN) and the overweight comparison (OP/ON); five of these exhibited inverse expression patterns in the two groups (*MTRF1L*, *HNRPD*, *ROBO3*, *FTO* and *SQSTM1*). Hundred and twenty-five DEGs were found in the comparison of overweight non-PCOS with lean non-PCOS (ON/LN), 51 of those genes overlapped with the group of DEGs that resulted from the comparison of lean PCOS with the lean non-PCOS. The comparison of all overweight with all lean patients yielded only 12 genes, all of which had a fold change lower than two.

Quantitative PCR

To validate the microarray data, five of the DEGs were chosen for validation by qPCR: *MRO*, *HAPLN1*, *OGT*, *CALR* and *FLNA* (Fig. 2). The criteria for their selection were a high FC value in one of the groups and the relevance of the gene to future study of PCOS pathogenesis. For all five genes, the qPCR results were in line with the microarray data. Interestingly, the differential expression of *MRO* demonstrated by qPCR was not as prominent as in the microarray. PCR analysis using primers for exons 4–9 (data not shown), following sequencing, revealed multiple splice variants. The full transcript exhibited significantly higher expression in the LP group. The significance of this finding and its potential role in PCOS pathology are currently under investigation.

Discussion

This is the first report of differential gene expression profiles in cultured cumulus cells taken from PCOS and non-PCOS patients. The comparison involved a homogeneous group of PCOS patients and controls, testing of specific and unique synchronized cells under identical culture conditions. We chose to analyze cumulus cells despite their relatively smaller number in comparison with other follicular cells for several reasons: cumulus cells are a unique subset of granulosa cells that are in direct contact with the oocyte throughout its development. These cells play a major role in the control of oocyte metabolism, and therefore it is likely that malfunction of these cells might play a role in PCOS. Moreover, due to the method of separation, the cumulus cells are more homogeneous with almost no contamination with other cells. Granulosa cells on the other hand, despite meticulous efforts to isolate them, would generally contain theca and blood cells. Homogeneity of the examined tissue is crucial for a valid comparison of gene expression.

The cells were retrieved with the oocytes following intense ovarian stimulation, as part of an IVF procedure. The separation of the cumulus cells from the oocyte was done with a combination of a short exposure to hyaluronidase and mechanical stripping. We decided to culture the cumulus cells for 48 h under identical conditions in order to achieve homogeneous extracellular environment, attenuating the effects of the hormonal stimulation and stripping. We hypothesized that differences in gene expression under controlled and identical conditions will most probably be weaker but would best reflect differences that arise from the cells' unique innate function. The manipulations to which the cumulus cells were exposed most probably affected their gene expression; however, as cells of all experimental groups underwent the same identical procedures, it is unlikely that these manipulations are the cause of the differential gene expression patterns.

The following discussion relates to the list of DEGs with a $|FC| \geqslant 1.5$, which provides a detailed comparison of the groups. Despite the relatively large number of DEGs, choosing a higher FC would have resulted in a loss of a significant amount of information mainly in overlapping genes and gene pathways. We included DEGs with |FC| higher than two in Table A1 only due to the length of the original list of genes. The two comparisons that showed the largest number of DEGs were the lean PCOS versus lean controls (487) and the overweight PCOS versus lean PCOS (305). The comparison of overweight PCOS with overweight controls resulted in a smaller number of DEGs (174). Comparison of the entire group of PCOS patients with the entire group of controls, irrespective of weight,

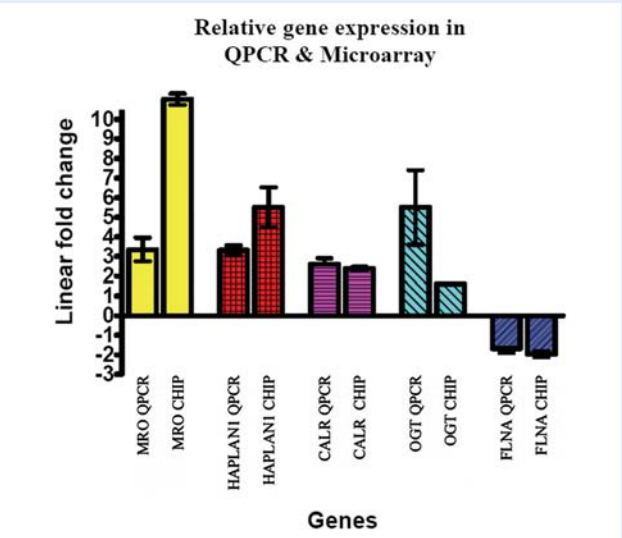

Figure 2 A histogram showing qPCR and microarray results for selected genes: *MRO* (maestro), *HAPLN1* (hyaluronan and proteoglycan link protein1), *CALR* (calreticulin), *OGT* (GlcNAc transferase) and *FLNA* (filamin A) compared with the GAPDH expression. The *Y*-axis represents relative linear fold change.

yielded the smallest group (109) of DEGs. These findings suggest that the most unique group in these comparisons was the lean PCOS. The expression of the genes in this group's cumulus cells was very different from both the overweight PCOS and the same-weight controls. The smaller number of differential genes in the more general comparison of all PCOS with all controls suggests that when weight is disregarded, the difference between PCOS and non-PCOS cumulus cells becomes less pronounced. Furthermore, the cumulus cells from the overweight PCOS group were most similar in terms of gene expression pattern to the cumulus cells of overweight controls. Taken together, it may be suggested that the lean PCOS group is the source of the unique characteristics of 'authentic' PCOS, while there is a similarity in cumulus cell function in the overweight patients of both groups. Moreover, the list of DEGs from the LP/LN and OP/LP comparisons contained 85 overlapping genes. This may suggest that the groups being compared with the lean PCOS group are not as different from one another.

In recent years, there have been a number of studies suggesting similarities in pathogenesis between obesity and PCOS (Morales *et al*., 1996; San Millan *et al*., 2004; Magnotti and Futterweit, 2007). Other studies have highlighted the differences that exist between lean and obese PCOS patients, demonstrating higher levels of basal LH, as was shown in this study, and a higher LH response to GnRH (Dale *et al*., 1992) as well as a higher growth hormone pulse amplitude in lean PCOS. In contrast, obese PCOS individuals demonstrated a higher rate of insulin resistance and the presence of β-cell dysfunction, lower levels of sex hormone binding globulin (SHBG), lower concentration of the insulin-like growth factor binding protein 1 (IGFBP1), and higher ratio of estradiol and testosterone to SHBG (Morales *et al*., 1996). The recent increase in the incidence of obesity worldwide has been accompanied by a parallel increase in the incidence of anovulatory infertility due to PCOS (Alvarez-Blasco *et al*., 2006). Furthermore, the first line of treatment for overweight PCOS is weight reduction, which has proven to be an effective treatment for resumption of ovulation (Guzick, 2007).

The analysis of gene annotations in this study resulted in the identification of several important pathways and groups of genes that shed light on molecular processes in PCOS. Genes of the Wnt/β-catenin- and MAPK-signaling pathways were generally down-regulated in the lean PCOS group when compared with PCOS controls. Wnts are secreted extracellular signaling molecules that exert local control over diverse developmental processes, cell-fate specification, differentiation and regulation of cell-to-cell interactions through β-catenin. Together with the MAPK-signaling pathway, they are known to function in gender differentiation, folliculogenesis and ovulation (Richards *et al*., 2002). For example, *TCF7L2*, a transcription factor in the Wnt pathway whose expression was lower in lean PCOS cells compared with lean controls, forms a complex with the androgen receptor (AR) and β-catenin, providing a mechanism for cooperative and selective gene regulation by AR and the Wnt/β-catenin-Tcf pathway (Amir *et al*., 2003). Several studies described altered expression of a few members of the Wnt and MAPK pathways in other cell types of PCOS patients (Jansen *et al*., 2004; Wood *et al*., 2004; Corton *et al*., 2006). It should be noted that each of those studies examined different tissues at different stages of the menstrual cycle. Another group of DEGs that were prominent in the comparison of lean PCOS with lean controls were genes encoding proteins of the extracellular matrix and proteins with significant roles in *O*- and *N*-glycosylation (a key step in extracellular-matrix assembly). The extracellular matrix plays a major role in folliculogenesis (reviewed in Irving-Rodgers, 2005). For example, transcript levels of the hyaluronan and proteoglycan link protein 1 (*HAPLN1*) were significantly up-regulated in the lean PCOS group. HAPLN1 is induced by gonadotrophins and plays an important role in cumulus expansion; this finding might explain in part the increased responsiveness of PCOS cumulus cells to gonadotrophins (Kobayashi *et al*., 1999).

The comparison of overweight PCOS versus overweight controls yielded a group of genes related to the insulin-signaling system whose transcript levels were up-regulated in the OP group. Among them are *INSR*, *IRS1* and the fat-mass and obesity-associated gene (*FTO*), whose variant rs9939609 has been shown to be associated with PCOS (Barber *et al*., 2008). In the same comparison, down-regulation of transcript levels was demonstrated for a group of genes encoding components of the cells energy system signaling, such as proteins of the mitochondrion, the oxidative phosphorylation system and biosynthesis of purines and pyrimidines.

Concluding remarks

Our results support the largely accepted tenet that PCOS patients who do not suffer from the co-morbidity of obesity represent the authentic syndrome with its unique characteristics. Obesity may be regarded as modifier of the syndrome or as a separate pathological mechanism that results in similar consequences. Analyses of individual gene expression levels at the mRNA level are always prone to personal variation. The fact that comparison of the entire PCOS group with healthy controls (without taking BMI into consideration) revealed significantly less DEGs, implies that grouping the individuals according to BMI reduces variability. Thus, our data support previous notions that PCOS in lean and obese individuals should be regarded as separate subentities. Further large-scale molecular studies and subgrouping PCOS patients into more homogeneous groups may provide a better understanding of the molecular pathophysiology of this syndrome.

Acknowledgements

The authors thank Yael Sunin, Sarit Albuteino, Iris Har-Vardi and Tatiana Rabinski for their excellent technical assistance.

Funding

This work was supported by the Ben-Gurion University Faculty of Health Sciences research fund (to Y.B., S.K., G.P. and O.S.B), NIBN research grant (S.K. and O.S.B) and the Morris Kahn Family Foundation for Humanitarian Support.

References

Agrawal R, Jacobs H, Payne N, Conway G. Concentration of vascular endothelial growth factor released by cultured human luteinized granulosa cells is higher in women with polycystic ovaries than in women with normal ovaries. *Fertil Steril* 2002;**78**:1164–1169.

Alvarez-Blasco F, Botella-Carretero JI, San Millan JL, Escobar-Morreale HF. Prevalence and characteristics of the polycystic ovary syndrome in overweight and obese women. *Arch Intern Med* 2006;**166**:2081–2086.

Amir AL, Barua M, McKnight NC, Cheng S, Yuan X, Balk SP. A direct β-catenin-independent interaction between androgen receptor and T cell factor 4. *J Biol Chem* 2003;**278**:30828–30834.

Barber TM, Bennett AJ, Groves CJ, Sovio U, Ruokonen A, Martikainen H, Pouta A, Hartikainen AL, Elliott P, Lindgren CM *et al.* Association of variants in the fat mass and obesity associated (FTO) gene with polycystic ovary syndrome. *Diabetologia* 2008;**51**:1153–1158.

Corton M, Botella-Carretero JI, Benguria A, Villuendas G, Zaballos A, San Millan JL, Escobar-Morreale HF, Peral B. Differential gene expression profile in omental adipose tissue in women with polycystic ovary syndrome. *J Clin Endocrinol Metab* 2007;**92**:328–337.

Dale PO, Tanbo T, Vaaler S, Abyholm T. Body weight, hyperinsulinemia, and gonadotropin levels in the polycystic ovarian syndrome: evidence of two distinct populations. *Fertil Steril* 1992;**58**:487–491.

Diamanti-Kandarakis E, Piperi C. Genetics of polycystic ovary syndrome: searching for the way out of the labyrinth. *Hum Reprod Update* 2005; **11**:631–643.

Escobar-Morreale HF, Luque-Ramirez M, San Millan JL. The molecular-genetic basis of functional hyperandrogenism and the polycystic ovary syndrome. *Endocr Rev* 2005;**26**:251–282.

Fleige S, Walf V, Huch S, Prgomet C, Sehm J, Pfaffl MW. Comparison of relative mRNA quantification models and the impact of RNA integrity in quantitative real-time RT–PCR. *Biotechnol Lett* 2006;**28**:1601–1613.

Franks S. Polycystic ovary syndrome. *N Engl J Med* 1995;**333**:853–861.

Franks S, McCarthy MI, Hardy K. Development of polycystic ovary syndrome: involvement of genetic and environmental factors. *Int J Androl* 2006;**29**:278–285. (Discussion 86–90).

Geary S, Moon YS. The human embryo *in vitro*: recent progress. *J Reprod Med* 2006;**51**:293–302.

Guzick DS. Ovulation induction management of PCOS. *Clin Obstet Gynecol* 2007;**50**:255–267.

Hickey TE, Legro RS, Norman RJ. Epigenetic modification of the X chromosome influences susceptibility to polycystic ovary syndrome. *J Clin Endocrinol Metab* 2006;**91**:2789–2791.

Irizarry RA, Hobbs B, Collin F, Beazer-Barclay YD, Antonellis KJ, Scherf U, Speed TP. Exploration, normalization, and summaries of high density oligonucleotide array probe level data. *Biostatistics* 2003;**4**:249–264.

Irving-Rodgers HF, Rodgers RJ. Extracellular matrix in ovarian follicular development and disease. *Cell Tissue Res* 2005;**322**:89–98.

Jansen E, Laven JS, Dommerholt HB, Polman J, van Rijt C, van den Hurk C, Westland J, Mosselman S, Fauser BC. Abnormal gene expression profiles in human ovaries from polycystic ovary syndrome patients. *Mol Endocrinol* 2004;**18**:3050–3063.

Kobayashi H, Sun GW, Hirashima Y, Terao T. Identification of link protein during follicle development and cumulus cell cultures in rats. *Endocrinology* 1999;**140**:3835–3842.

Legro RS, Driscoll D, Strauss JF 3rd, Fox J, Dunaif A. Evidence for a genetic basis for hyperandrogenemia in polycystic ovary syndrome. *Proc Natl Acad Sci USA* 1998;**95**:14956–14960.

Magnotti M, Futterweit W. Obesity and the polycystic ovary syndrome. *Med Clin North Am* 2007;**91**:1151–1168, ix–x.

Morales AJ, Laughlin GA, Butzow T, Maheshwari H, Baumann G, Yen SS. Insulin, somatotropic, and luteinizing hormone axes in lean and obese women with polycystic ovary syndrome: common and distinct features. *J Clin Endocrinol Metab* 1996;**81**:2854–2864.

Okamura-Oho Y, Miyashita T, Ohmi K, Yamada M. Dentatorubral-pallidoluysian atrophy protein interacts through a proline-rich region near polyglutamine with the SH3 domain of an insulin receptor tyrosine kinase substrate. *Hum Mol Genet* 1999;**8**:947–957.

Oksjoki S, Soderstrom M, Inki P, Vuorio E, Anttila L. Molecular profiling of polycystic ovaries for markers of cell invasion and matrix turnover. *Fertil Steril* 2005;**83**:937–944.

Oliveros JC. VENNY. An interactive tool for comparing lists with Venn Diagrams. 2007. http://bioinfogp.cnb.csic.es/tools/venny/index.html.

Pfaffl MW. A new mathematical model for relative quantification in real-time RT–PCR. *Nucleic Acids Res* 2001;**29**:e45.

Quinn MC, McGregor SB, Stanton JL, Hessian PA, Gillett WR, Green DP. Purification of granulosa cells from human ovarian follicular fluid using granulosa cell aggregates. *Reprod Fertil Dev* 2006;**18**:501–508.

Rice S, Christoforidis N, Gadd C, Nikolaou D, Seyani L, Donaldson A, Margara R, Hardy K, Franks S. Impaired insulin-dependent glucose metabolism in granulosa-lutein cells from anovulatory women with polycystic ovaries. *Hum Reprod* 2005;**20**:373–381.

Richards JS, Russell DL, Ochsner S, Hsieh M, Doyle KH, Falender AE, Lo YK, Sharma SC. Novel signaling pathways that control ovarian follicular development, ovulation, and luteinization. *Recent Prog Horm Res* 2002;**57**:195–220.

Salehi M, Bravo-Vera R, Sheikh A, Gouller A, Poretsky L. Pathogenesis of polycystic ovary syndrome: what is the role of obesity? *Metabolism* 2004; **53**:358–376.

Sam S, Dunaif A. Polycystic ovary syndrome: syndrome XX? *Trends Endocrinol Metab* 2003;**14**:365–370.

San Millan JL, Corton M, Villuendas G, Sancho J, Peral B, Escobar-Morreale HF. Association of the polycystic ovary syndrome with genomic variants related to insulin resistance, type 2 diabetes mellitus, and obesity. *J Clin Endocrinol Metab* 2004;**89**:2640–2646.

Smyth GK. Linear models and empirical bayes methods for assessing differential expression in microarray experiments. *Stat Appl Genet Mol Biol* 2004;**3**:Article 3.

Speroff L, Fritz MA. *Clinical Gynecologic Endocrinology and Infertility*, Vol. **x**, 7th edn. Philadelphia: Lippincott Williams & Wilkins, 2005, 1334 p.

Stewart DR, Dombroski BA, Urbanek M, Ankener W, Ewens KG, Wood JR, Legro RS, Strauss JF 3rd, Dunaif A, Spielman RS. Fine mapping of genetic susceptibility to polycystic ovary syndrome on chromosome 19p13.2 and tests for regulatory activity. *J Clin Endocrinol Metab* 2006;**91**:4112–4117.

Vink JM, Sadrzadeh S, Lambalk CB, Boomsma DI. Heritability of polycystic ovary syndrome in a Dutch twin-family study. *J Clin Endocrinol Metab* 2006;**91**:2100–2104.

Wood JR, Ho CK, Nelson-Degrave VL, McAllister JM, Strauss JF 3rd. The molecular signature of polycystic ovary syndrome (PCOS) theca cells defined by gene expression profiling. *J Reprod Immunol* 2004;**63**:51–60.

Wood JR, Dumesic DA, Abbott DH, Strauss JF 3rd. Molecular abnormalities in oocytes from women with polycystic ovary syndrome revealed by microarray analysis. *J Clin Endocrinol Metab* 2007; **92**:705–713.

Appendix

Table AI The DEGs with FC ⩾ |2| and *P*-value <0.01 in six comparisons: (LP/LN) lean PCOS versus lean controls; (OP/ON) overweight PCOS versus overweight controls; (PS/NP) all PCOS versus all controls; (OP/LP) overweight PCOS versus lean PCOS; (ON/LN) overweight non-PCOS versus lean non-PCOS; (O/L) overweight versus lean

Probe set ID	Gene title	Gene symbol	Chromosomal location	LP/LN *P*-value	FC	OP/ON *P*-value	FC	PS/NP *P*-value	FC	ON/LN *P*-value	FC	OP/LP *P*-value	FC	O/L *P*-value	FC	Gene annotation codes
202323_s_at	Acyl-co-enzyme A binding domain containing 3	ACBD3	Chr1q42.12	0.007	−2.26	0.964		0.098		0.571		0.020		0.320		34,35,36
228771_at	Adrenergic, beta, receptor kinase 2	ADRBK2	Chr22q11-12.1	0.109		0.194		0.680		0.007	−2.17	0.995		0.054		6,10,14,16
228667_at	1-Acylglycerol-3-phosphate *O*-acyltransferase 4	AGPAT4	Chr6q26	0.000	−3.92	0.344		0.045		0.019		0.002	2.55	0.758		35
205609_at	Angiopoietin 1	ANGPT1	Chr8q22.3-q23	0.005	2.21	0.619		0.195		0.732		0.003	−2.29	0.100		14,24,27
236034_at	Microcephaly, primary autosomal recessive 1	ANGPT2	Chr8p23.1	0.011		0.075		0.002	2.35	0.384		0.949		0.405		14,24,27
210143_at	Annexin A10	ANXA10	Chr4q33	0.001	2.51	0.864		0.031		0.058		0.051		0.850		49
201613_s_at	Adaptor-related protein complex 1, gamma 2 subunit 1	AP1G2	Chr14q11.2	0.004	−2.16	0.446		0.124		0.025		0.112		0.550		22,47
224797_at	Arrestin domain containing 3	ARRDC3	Chr5q14.3	0.007	2.41	0.487		0.013		0.053		0.781		0.183		18
214012_at	Type 1 tumor necrosis factor receptor shedding aminopeptidase regulator	ARTS-1	Chr5q15	0.104		0.542		0.748		0.428		0.004	−3.07	0.012		13,25,26,27,46
209935_at	ATPase, Ca^{++} transporting, type 2C, member 1	ATP2C1	Chr3q22.1	0.081		0.226		0.893		0.772		0.010	−2.19	0.103		9,16,36,37,49
214594_x_at	ATPase, Class I, type 8B, member 1	ATP8B1	Chr18q21-31	0.014		0.031		0.971		0.291		0.001	2.18	0.096		3,16
225606_at	BCL2-like 11 (apoptosis facilitator)	BCL2L11	Chr2q13	0.008	−2.06	0.499		0.016		0.043		0.926		0.132		17
200056_s_at	Nuclear DNA-binding protein	C1D	Chr2p13-p12	0.676		0.004	2.48	0.039		0.018		0.907		0.246		3,17,19
224444_s_at	Chromosome 1 open reading frame 97	C1orf97	Chr1q32.3	0.004	2.06	0.028		0.799		0.115		0.001	−2.39	0.205		—
219004_s_at	Chromosome 21 open reading frame 45	C21orf45	Chr21q22.11	0.001	−2.20	0.663		0.007	−1.56	0.019		0.324		0.261		—
242418_at	Transcribed locus	C2orf27	—	0.035		0.081		0.939		0.257		0.008	2.10	0.267		—
217767_at	Complement component 3	C3	Chr19p13.3-p13.2	0.009	3.30	0.728		0.134		0.272		0.044		0.640		14,27,28,49
236826_at	Chromosome 9 open reading frame 52	C9orf52	Chr9p22.3	0.007	2.05	0.664		0.043		0.635		0.047		0.445		—
227623_at	Calcium channel, voltage-dependent, alpha 2/ delta subunit 1	CACNA2D1	Chr7q21-q22	0.014		0.005	2.24	0.000	2.17	0.781		0.509		0.352		2,49
34726_at	Calcium channel, voltage-dependent, beta 3 subunit	CACNB3	Chr12q13	0.001	−2.37	0.034		0.372		0.002	−2.19	0.015		0.589		2,16,49
212952_at	Calreticulin	CALR*	Chr19p13.3-2	0.009	2.29	0.784		0.035		0.079		0.442		0.377		3,17,21,26,37
214316_x_at	Calreticulin	CALR*	Chr19p13.3-3	0.008	2.46	0.264		0.007	1.86	0.237		0.534		0.512		3,17,2,26,37
210026_s_at	Caspase recruitment domain family, member 10	CARD10	Chr22q13.1	0.462		0.005	2.52	0.146		0.035		0.134		0.836		9,17,22
205476_at	Chemokine (C-C motif) ligand 20	CCL20	Chr2q33-q37	0.003	4.99	0.177		0.311		0.087		0.007	−4.05	0.545		14,15,27,28
200951_s_at	Cyclin D2	CCND2	Chr12p13	0.068		0.040		0.005	−2.03	0.985		0.851		0.663		1,5,31
232266_x_at	Cell division cycle 2-like 5	CDC2L5	Chr7p13	0.008	−1.70	0.042		0.873		0.281		0.001	2.04	0.100		5
203468_at	Cyclin-dependent kinase (CDC2-like) 10	CDK10	Chr16q24	0.003	−2.07	0.812		0.046		0.018		0.290		0.281		5
213348_at	Cyclin-dependent kinase inhibitor 1C (p57, Kip2)	CDKN1C	Chr11p15.5	0.001	−3.05	0.487		0.057		0.017		0.039		0.678		3,4,5, 7

Continued

Table AI *Continued*

Probe set ID	Gene title	Gene symbol	Chromosomal location	LP/LN *P*-value	FC	OP/ON *P*-value	FC	PS/NP *P*-value	FC	ON/LN *P*-value	FC	OP/LP *P*-value	FC	O/L *P*-value	FC	Gene annotation codes
236313_at	Cyclin-dependent kinase inhibitor 2B (p15)	CDKN2B	Chr9p21	0.014		0.158		0.008	2.04	0.872		0.269		0.775		5,6,7,43
214907_at	Carcinoembryonic antigen-related cell adhesion molecule 21	CEACAM21	Chr19q13.2	0.001	−4.47	0.268		0.003	−2.59	0.234		0.172		0.827		12
239413_at	KIAA0912 protein	CEP152	Chr15q21.1	0.004	−2.10	0.347		0.007	−1.62	0.162		0.413		0.509		—
219867_at	Chondrolectin	CHODL	Chr21q11.2	0.010	−2.91	0.554		0.025		0.319		0.216		0.927		24
219634_at	Carbohydrate (chondroitin 4) sulfotransferase 11	CHST11	Chr12q	0.003	2.43	0.881		0.030		0.094		0.171		0.663		32,52
226736_at	Churchill domain containing 1	CHURC1	Chr14q23.3	0.004	−3.87	0.179		0.003	−2.61	0.263		0.466		0.571		3
219866_at	Chloride intracellular channel 5	CLIC5	Chr6p12.1-21.1	0.010	2.20	0.054		0.002	1.93	0.881		0.483		0.980		37,48
206818_s_at	Cyclin M2	CNNM2	Chr10q24.33	0.001	−2.18	0.129		0.001	−1.81	0.013		0.548		0.034		37,48
217428_s_at	Collagen, type X, alpha 1	COL10A1	Chr6q21-q22	0.919		0.008	5.31	0.066		0.137		0.172		0.865		30,49
222008_at	Collagen, type IX, alpha 1	COL9A1	Chr6q12-q14	0.008	−2.01	0.190		0.004	−1.69	0.101		0.915		0.164		3,12,46
1556346_at	Coactosin-like 1 (Dictyostelium)	COTL1	Chr16q24.1	0.425		0.005	−2.23	0.015		0.093		0.662		0.634		37
225129_at	Copinell	CPNE2	Chr16q13	0.005	−2.23	0.948		0.037		0.040		0.373		0.323		
228318_s_at	Cysteine-rich PAK1 inhibitor	CRIPAK	Chr4p16.3	0.008	−2.72	0.348		0.228		0.056		0.072		0.848		37,39,50
209981_at	Cold shock domain containing C2, RNA binding	CSDC2	Chr22q13.2-31	0.005	−2.30	0.537		0.143		0.127		0.039		0.829		3,20,59
206754_s_at	Cytochrome P450, family 2, subfamily B, polypeptide 7 pseudogene 1	CYP2B7P1	Chr19q13.2	0.086		0.005	2.72	0.390		0.033		0.015		0.716		—
209569_x_at	DNA segment on chromosome 4 (unique) 234 expressed sequence	D4S234E	Chr4p16.3	0.353		0.006	−2.26	0.197		0.039		0.098		0.932		
226666_at	Dishevelled associated activator of morphogenesis 1	DAAM1	Chr14q23.1	0.010	−2.23	0.421		0.202		0.056		0.109		0.732		1,37
232552_at	cDNA DKFZp686E17205	DAAM1	—	0.000	−2.24	0.721		0.033		0.109		0.004	1.77	0.543		1,37
219179_at	Dapper, antagonist of β-catenin, homolog 1 (*Xenopus laevis*)	DACT1	Chr14q23.1	0.007	−2.59	0.108		0.393		0.004	−2.85	0.182		0.245		1
213865_at	Discoidin, CUB and LCCL domain containing 2	DCBLD2	Chr3q12.1|3	0.431		0.002	−1.91	0.190		0.001	2.09	0.741		0.074		12
207169_x_at	Discoidin domain receptor family, member 1	DDR1	Chr6p21.3	0.006	−2.16	0.608		0.019		0.132		0.310		0.565		12,13,16
227199_at	DIP2 disco-interacting protein 2 homolog A (Drosophila)	DIP2A	Chr21q22.3	0.002	−2.00	0.175		0.207		0.007	−1.80	0.064		0.481		3,36
214724_at	DIX domain containing 1	DIXDC1	—	0.009	−2.01	0.779		0.034		0.035		0.730		0.164		1,37
202843_at	DnaJ (Hsp40) homolog, subfamily B, member 9	DNAJB9	Chr7q31	0.121		0.913		0.558		0.271		0.008	−2.07	0.011		21,53
235341_at	DnaJ (Hsp40) homolog, subfamily C, member 3	DNAJC3	Chr13q32	0.000	3.09	0.599		0.002	1.83	0.029		0.027		0.759		21,53
227084_at	Dystrobrevin, alpha	DTNA	Chr18q12	0.010	−2.03	0.159		0.416		0.041		0.044		0.930		14,16
211200_s_at	EF-hand calcium binding domain 2	EFCAB2	Chr1q44	0.008	2.52	0.550		0.162		0.140		0.054		0.868		—
223608_at	EF-hand calcium binding domain 2	EFCAB2	Chr1q44	0.005	2.79	0.490		0.168		0.172		0.023		0.627		—
222938_x_at	Ectonucleotide pyrophosphatase/ phosphodiesterase 3	ENPP3	Chr6q22	0.000	3.16	0.048		0.000	2.31	0.298		0.249		0.735		16,36,38
205225_at	Estrogen receptor 1	ESR1	Chr6q25.1	0.004	−2.28	0.635		0.015		0.025		0.703		0.148		3,8,14

232174_at	Exostoses (multiple) 1	EXT1	Chr8q24.11-13	0.020		0.050		0.971		0.258		0.002	2.30	0.167	5,54
237310_at	Exostoses (multiple) 1	EXT1	Chr8q24.11	0.021		0.010		0.624		0.702		0.000	2.42	0.011	5,54
239227_at	Exostoses (multiple) 1	EXT1	Chr8q24.11-13	0.039		0.154		0.831		0.526		0.006	2.01	0.133	5,54
221959_at	Family with sequence similarity 110, member B	FAM110B	Chr8q12.1	0.616		0.002	2.09	0.057		0.146		0.024		0.421	—
228790_at	Family with sequence similarity 110, member B	FAM110B	Chr8q12.1	0.509		0.008	2.28	0.126		0.225		0.030		0.382	—
57715_at	Family with sequence similarity 26, member B	FAM26B	Chr10pter-q26.12	0.000	−2.12	0.636		0.031		0.002	−1.90	0.282		0.128	—
227948_at	FYVE, RhoGEF and PH domain containing 4	FGD4	Chr12p11.21	0.015		0.087		0.712		0.130		0.008	2.54	0.434	37
1557385_at	Hypothetical protein FLJ13305	FLJ13305	Chr2p15	0.001	−2.08	0.313		0.002	−1.61	0.018		0.637		0.147	—
225035_x_at	CXYorf1-related protein	FLJ25222	ChrXq28;Yq12 /chr	0.005	−2.29	0.918		0.055		0.090		0.149		0.709	
226340_x_at	CXYorf1-related protein	FLJ25222		0.002	−2.18	0.748		0.059		0.065		0.077		0.802	
233929_x_at	CXYorf1-related protein	FLJ25222		0.007	−2.18	0.950		0.053		0.159		0.151		0.848	
200859_x_at	Filamin A, alpha (actin binding protein 280)	FLNA	ChrXq28	0.004	−2.12	0.980		0.059		0.360		0.031		0.537	3,8,9,24,37
1558199_at	Fibronectin 1	FN1	Chr2q34	0.009	−3.06	0.471		0.222		0.232		0.023		0.537	12,30
202723_s_at	Forkhead box O1A (rhabdomyosarcoma)	FOXO1A	Chr13q14.1	0.004	−2.02	0.774		0.027		0.182		0.112		0.940	3,4,18
232882_at	Forkhead box O1A/membrane-associated guanylate kinase	FOXO1A	Chr13q14.1	0.010	−2.30	0.995		0.108		0.661		0.022		0.285	3,4,18
202748_at	Guanylate binding protein 2, interferon inducible	GBP2	Chr1p22.2	0.005	2.09	0.324		0.007	1.62	0.169		0.443		0.496	27
213713_s_at	Galactosidase, beta 1-like 2	GLB1L2	Chr11q25	0.001	−2.30	0.764		0.032		0.036		0.043		0.784	32
204187_at	Guanosine monophosphate reductase	GMPR	Chr6p23	0.006	−2.23	0.399		0.011		0.218		0.344		0.642	38
215203_at	Golgi autoantigen, golgin subfamily a, 4	GOLGA4	Chr3p22-p21.3	0.002	−2.23	0.549		0.081		0.058		0.034		0.975	16
220993_s_at	G protein-coupled receptor 63	GPR63	Chr6q16.1-q16.3	0.015		0.157		0.005	−2.08	0.323		0.841		0.419	14/10
223582_at	Monogenic, audiogenic seizure susceptibility 1 homolog	GPR98	Chr5q13	0.004	3.57	0.485		0.128		0.057		0.063		0.850	14/10
226606_s_at	GTP binding protein 5 (putative)	GTPBP5	Chr20q13.33	0.920		0.020		0.063		0.656		0.009	−2.32	0.023	16,23
205523_at	Hyaluronan and proteoglycan link protein 1	HAPLN1	Chr5q14.3	0.003	7.37	0.330		0.007	3.48	0.359		0.153		0.986	12,30
205524_s_at	Hyaluronan and proteoglycan link protein 1	HAPLN1		0.001	3.84	0.825		0.015		0.065		0.112		0.672	12,30
230204_at	Hyaluronan and proteoglycan link protein 1	HAPLN1		0.006	5.30	0.255		0.006	3.11	0.282		0.397		0.652	12,30
241710_at	Transcribed locus	hCG_1645220	—	0.047		0.486		0.566		0.852		0.006	−2.06	0.046	—
202455_at	Histone deacetylase 5	HDAC5	Chr17q21	0.000	−2.89	0.562		0.028		0.008	−1.98	0.034		0.563	3,5,40
242317_at	Transcribed locus	HIGD1A	—	0.010	2.41	0.583		0.204		0.379		0.018		0.376	—
235456_at	Histone 1, H2bd	HIST1H2BD	Chr6p21.3	0.017		0.016		0.001	2.10	0.738		0.705		0.971	40
232035_at	Histone 1, H4 h	HIST1H4H	Chr6p21.3	0.019		0.040		0.933		0.078		0.009	−2.04	0.520	40
214290_s_at	Histone cluster 2, H2aa3/4	HIST2H2AA	Chr1q21.2	0.006	2.93	0.065		0.566		0.027		0.016		0.910	40
218280_x_at	Histone cluster 2, H2aa3/5	HIST2H2AA	Chr1q21.3	0.004	2.50	0.058		0.514		0.020		0.012		0.924	
227943_at	Histone 2, H2aa	HIST2H2AA	Chr1q21.4	0.002	2.30	0.219		0.003	1.71	0.517		0.090		0.760	
227614_at	Hexokinase domain containing 1	HKDC1	Chr10q22.1	0.006	2.82	0.458		0.026		0.872		0.035		0.322	6,16
213359_at	Heterogeneous nuclear ribonucleoprotein D	HNRPD	Chr4q21.1-2	0.008	−2.77	0.005	2.86	0.950		0.002	−3.56	0.029		0.526	3,16,19
241702_at	Heterogeneous nuclear ribonucleoprotein D	HNRPD	Chr4q21.1-2	0.007	−2.92	0.609		0.114		0.039		0.204		0.481	3,16,19
231050_at	H-rev107-like protein 5	HRASLS5	Chr11q13.2	0.000	3.99	0.942		0.024		0.153		0.007	−2.53	0.584	
221771_s_at	M-phase phosphoprotein, mpp8	HSMPP8	Chr13q12.11	0.000	−1.81	0.114		0.142		0.000	−2.07	0.503		0.019	5,40
237377_at	Insulin-like growth factor 1 receptor	IGF1R	Chr15q26.3	0.004	−2.40	0.038		0.639		0.025		0.007	2.23	0.747	14,16,24,18
213792_s_at	Insulin receptor	INSR	Chr19p13.3-13.2	0.207		0.001	2.60	0.093		0.107		0.001	2.37	0.194	14,18,24,32

Continued

Table AI *Continued*

Probe set ID	Gene title	Gene symbol	Chromosomal location	LP/LN *P*-value	FC	OP/ON *P*-value	FC	PS/NP *P*-value	FC	ON/LN *P*-value	FC	OP/LP *P*-value	FC	O/L *P*-value	FC	Gene annotation codes
226216_at	Insulin receptor	INSR		0.773		0.009	2.69	0.075		0.469		0.026		0.208		14,18,24, 32
204686_at	Insulin receptor substrate 1	IRS1	Chr2q36	0.817		0.001	2.59	0.015		0.036		0.218		0.818		14,18,24,32
225390_s_at	Kruppel-like factor 13	KLF13	Chr15q12	0.001	−2.23	0.076		0.001	−1.76	0.574		0.130		0.870		3,4
219331_s_at	Kelch domain containing 8A	KLHDC8A	Chr1q32.1	0.006	−3.14	0.655		0.022		0.132		0.291		0.585		—
221221_s_at	Kelch-like 3 (Drosophila)	KLHL3	Chr5q31	0.449		0.008	2.30	0.168		0.063		0.104		0.964		29
209894_at	Leptin receptor	LEPR	Chr1p31	0.750		0.005	2.00	0.098		0.002	−2.25	0.401		0.023		36,37,35
223828_s_at	Lectin, galactoside-binding, soluble, 12	LGALS12	Chr11q13	0.003	5.31	0.541		0.020		0.556		0.042		0.508		17
207240_s_at	Luteinizing hormone/choriogonadotrophin receptor	LHCGR	Chr2p21	0.006	2.98	0.188		0.005	2.14	0.578		0.254		0.963		10,14,24
1558080_s_at	Hypothetical protein LOC144871	LOC144871	Chr13q32.1	0.000	3.46	0.618		0.001	1.90	0.024		0.004	−1.89	0.996		—
213089_at	Hypothetical protein LOC153561	LOC153561	Chr5q13.2	0.009	−2.22	0.778		0.063		0.656		0.037		0.381		—
211996_s_at	KIAA0220-like protein	LOC23117	Chr16p12.2	0.009	−2.53	0.931		0.088		0.291		0.068		0.736		—
225857_s_at	Hypothetical LOC388796	LOC388796	Chr20q11.23	0.004	−2.05	0.486		0.016		0.421		0.095		0.777		—
1558139_at	LOC440156	LOC440156	Chr14q11.1	0.002	−3.10	0.634		0.067		0.025		0.139		0.482		—
214373_at	Hypothetical gene supported by BC053580	LOC440996	Chr3q29	0.003	−2.16	0.653		0.065		0.018		0.200		0.361		—
209679_s_at	Small *trans*-membrane and glycosylated protein	LOC57228	Chr12q13.13	0.004	−2.15	0.121		0.002	−1.77	0.274		0.589		0.499		—
1557987_at	PI-3-kinase-related kinase SMG-1	LOC641298	Chr16p12.2	0.006	−2.85	0.167		0.350		0.036		0.034		0.946		—
1557360_at	Leucine-rich PPR-motif containing	LRPPRC	Chr2p21	0.008	−2.21	0.797		0.109		0.265		0.047		0.674		3,20
225474_at	Membrane associated guanylate kinase, WW and PDZ domain containing 1	MAGI1	Chr3p14.1	0.001	−2.55	0.084		0.272		0.020		0.003	2.13	0.727		1,9,12,13,17,22
242794_at	Mastermind-like 3 (Drosophila)	MAML3	Chr4q28	0.008	−2.00	0.171		0.389		0.047		0.036		0.994		3,4,11,24
212741_at	Monoamine oxidase A	MAOA	ChrXp11.3	0.014		0.059		0.622		0.003	−2.02	0.193		0.245		36
216237_s_at	MCM5 minichromosome maintenance deficient 5, cell division cycle 46	MCM5	Chr22q13.1	0.001	−2.79	0.430		0.005	−1.87	0.064		0.328		0.401		3,5,16,40
208795_s_at	MCM7 minichromosome maintenance deficient 7	MCM7	Chr7q21.3-q22.1	0.002	−2.36	0.625		0.011		0.033		0.476		0.241		3,5,16,40
210983_s_at	MCM7 minichromosome maintenance deficient 8	MCM7	Chr7q21.3-q22.1	0.002	−2.73	0.289		0.004	−1.99	0.026		0.980		0.100		3,5,16,40
239571_at	MADS box transcription enhancer factor 2, polypeptide A	MEF2A	Chr15q26.3	0.080		0.022		0.588		0.186		0.008	2.64	0.291		
223723_at	Antigen p97	MFI2	Chr3q28-q29	0.001	2.31	0.287		0.005	1.68	0.448		0.076		0.762		37,48
1565162_s_at	Microsomal glutathione *S*-transferase 1	MGST1	Chr12p12.3-p12.1	0.008	2.37	0.888		0.063		0.399		0.062		0.633		36
214246_x_at	Misshapen-like kinase 1 (zebrafish)	MINK1	Chr17p13.2	0.000	−2.73	0.171		0.088		0.001	−2.23	0.028		0.403		2,6,9,24
203414_at	Monocyte to macrophage differentiation-associated	MMD	Chr17q	0.001	3.23	0.896		0.032		0.108		0.026		0.861		—
1555741_at	Melanocortin 2 receptor accessory protein	MRAP	Chr21q22.1	0.006	2.33	0.858		0.045		0.250		0.102		0.919		—
224323_s_at	Maestro	MRO	Chr18q21	0.008	11.32	0.234		0.301		0.036		0.066		0.787		—
224324_at	Maestro	MRO	Chr18q21	0.008	10.73	0.185		0.348		0.031		0.057		0.798		—
204331_s_at	Mitochondrial ribosomal protein S12	MRPS12	Chr19q13.1-q13.2	0.929		0.002	−2.34	0.029		0.085		0.084		0.767		55, 56,57
225237_s_at	Musashi homolog 2 (Drosophila)	MSI2	Chr17q23.2	0.006	2.65	0.094		0.485		0.033		0.019		0.925		—

211783_s_at	Metastasis associated 1	MTA1	Chr14q32.3	0.009	−2.12	0.404		0.214		0.077		0.071		0.921	3,40
202555_s_at	Myosin, light polypeptide kinase	MYLK	Chr3q21	0.116		0.052		0.929		0.005	−2.13	0.611		0.115	6
242191_at	Neuroblastoma breakpoint family, member 11/10	NBPF11/ NBPF1	Chr1q21.1	0.002	−2.68	0.504		0.085		0.024		0.083		0.595	—
214693_x_at	Neuroblastoma breakpoint family, member14-20	NBPF14-20	Chr1q12-21/p36.13	0.028		0.508		0.439		0.956		0.006	2.56	0.074	—
213298_at	Nuclear factor 1/C (CCAAT-binding transcription factor)	NFIC	Chr19p13.3	0.007	−2.20	0.438		0.188		0.093		0.053		0.962	3,4
202237_at	Nicotinamide *N*-methyltransferase	NNMT	Chr11q23.1	0.026		0.085		0.004	2.88	0.637		0.880		0.599	35
202238_s_at	Nicotinamide *N*-methyltransferase	NNMT		0.022		0.080		0.004	2.95	0.647		0.832		0.629	35
228723_at	Neuroplastin	NPTN	Chr15q22	0.014		0.283		0.446		0.406		0.007	2.06	0.217	—
219147_s_at	Nicotinamide riboside kinases	NRK1	Chr9q21.13	0.147		0.013		0.616		0.001	−3.03	0.625		0.080	16,38
229225_at	Neuropilin 2	NRP2	Chr2q33.3	0.133		0.009	2.30	0.435		0.014		0.095		0.677	12, 25
200906_s_at	Palladin	PALLD	Chr4q32.3	0.004	−3.54	0.742		0.086		0.167		0.041		0.790	12,37
204715_at	Pannexin 1	PANX1	Chr11q21	0.006	2.16	0.725		0.088		0.068		0.146		0.666	—
226119_at	Protein-L-isoaspartate *O*-methyltransferase domain containing 1	PCMTD1	Chr8q11.23	0.735		0.008	2.14	0.104		0.052		0.255		0.750	
242844_at	Protein geranylgeranyltransferase type I, beta subunit	PGGT1B	Chr5q22.3	0.006	2.28	0.985		0.059		0.172		0.105		0.974	—
225321_s_at	Paired immunoglobin-like type 2 receptor beta	PILRB	Chr7q22.1	0.001	−2.81	0.379		0.125		0.067		0.013		0.780	—
203422_at	Polymerase (DNA directed), delta 1, catalytic subunit 125 kDa	POLD1	Chr19q13.3	0.002	−2.18	0.096		0.001	−1.79	0.107		0.808		0.250	5,38,40,41
219926_at	Popeye domain containing 3	POPDC3	Chr6q21	0.709		0.003	−2.06	0.016		0.148		0.166		0.786	—
226150_at	Phosphatidic acid phosphatase type 2 domain containing 1B	PPAPDC1B	Chr8p12	0.007	2.05	0.144		0.514		0.235		0.003	−2.18	0.241	3
209826_at	Palmitoyl-protein thioesterase 2/ EGF-like-domain, multiple 8	PPT2/EGFL8	Chr6p21.3-31	0.000	−2.21	0.507		0.064		0.068		0.007	1.73	0.711	24
235085_at	Homolog of rat pragma of Rnd2	PRAGMIN	Chr8p23.1	0.000	−2.05	0.177		0.000	−1.60	0.036		0.319		0.326	6,16
216881_x_at	Proline-rich protein BstNI subfamily 4	PRB4	Chr12p13.2	0.623		0.002	−2.05	0.087		0.010	1.82	0.286		0.445	10
201858_s_at	Proteoglycan 1, secretory granule	PRG1	Chr10q22.1	0.001	6.14	0.546		0.074		0.044		0.039		0.878	30
201859_at	Proteoglycan 1, secretory granule	PRG1	Chr10q22.1	0.004	3.67	0.804		0.063		0.061		0.148		0.628	30
226065_at	Prickle-like 1 (Drosophila)	PRICKLE1	Chr12q12	0.007	−2.71	0.269		0.285		0.074		0.034		0.891	1
213010_at	Protein kinase C, delta binding protein	PRKCDBP	Chr11p15.4	0.101		0.141		0.720		0.002	3.18	0.798		0.021	7
1558290_a_ at	Pvt1 oncogene homolog, MYC activator (mouse)	PVT1	Chr8q24.21	0.008	−2.21	0.882		0.075		0.106		0.171		0.720	—
206066_s_at	RAD51 homolog C (*Saccharomyces cerevisiae*)	RAD51C	Chr17q22-q23	0.152		0.001	−2.01	0.236		0.003	1.93	0.095		0.475	5
1557675_at	V-raf-1 murine leukemia viral oncogene homolog 1	RAF1	Chr3p25	0.001	−2.01	0.076		0.433		0.090		0.001	2.03	0.303	2,6,17,18,37
1553185_at	RAS and EF-hand domain containing	RASEF	Chr9q21.32	0.056		0.182		0.886		0.739		0.005	2.57	0.081	12,16,47,49
1553186_x_at	RAS and EF-hand domain containing	RASEF	Chr9q21.32	0.043		0.244		0.757		0.866		0.004	2.63	0.059	12,16,47,49
227223_at	RNA-binding region (RNP1, RRM) containing 2	RBM39	Chr20q11.22	0.012		0.053		0.847		0.221		0.002	2.53	0.178	3,19,20
238317_x_at	RNA binding motif, single stranded interacting protein 1	RBMS1	Chr2q24.2	0.005	2.84	0.205		0.007	2.01	0.811		0.119		0.610	—
228802_at	RNA binding protein with multiple splicing 2	RBPMS2	Chr15q22.31	0.003	−1.91	0.012		0.701		0.001	−2.03	0.024		0.501	—

Continued

Table AI *Continued*

Probe set ID	Gene title	Gene symbol	Chromosomal location	LP/LN *P*-value	FC	OP/ON *P*-value	FC	PS/NP *P*-value	FC	ON/LN *P*-value	FC	OP/LP *P*-value	FC	O/L *P*-value	FC	Gene annotation codes
222666_s_at	RNA terminal phosphate cyclase-like 1	RCL1	Chr9p24.1-p23	0.356		0.006	−2.26	0.016		0.053		0.990		0.360		23
205407_at	Reversion-inducing-cysteine-rich protein with kazal motifs	RECK	Chr9p13-p12	0.797		0.003	2.44	0.049		0.116		0.072		0.673		5, 30
226989_at	RGM domain family, member B	RGMB	Chr5q21.1	0.003	−2.50	0.703		0.063		0.025		0.191		0.413		3,11,12,14
220486_x_at	Transmembrane protein 164	RP13-360B22.2	ChrXq22.3	0.009	2.01	0.799		0.103		0.182		0.086		0.931		
236859_at	Runt-related transcription factor 2	RUNX2	Chr6p21	0.001	2.74	0.083		0.000	2.07	0.271		0.331		0.654		3,7
236858_s_at	Runt-related transcription factor 3	RUNX2	—	0.002	2.27	0.068		0.001	1.88	0.302		0.565		0.526		3,7
206306_at	Ryanodine receptor 3	RYR3	Chr15q14-q15	0.004	5.59	0.231		0.004	3.27	0.213		0.464		0.526		48
202036_s_at	Secreted frizzled-related protein 1	SFRP1	Chr8p12-p11.1	0.968		0.002	3.85	0.022		0.368		0.014		0.191		1,14,17
202037_s_at	Secreted frizzled-related protein 1	SFRP1	Chr8p12-p11.1	0.075		0.055		0.006	2.11	0.570		0.492		0.266		1,14,17
222310_at	Splicing factor, arginine/serine-rich 15	SFRS15	Chr21q22.1	0.009	−2.22	0.191		0.350		0.024		0.088		0.639		—
203889_at	Secretory granule, neuroendocrine protein 1	SGNE1	Chr15q13-q14	0.044		0.150		0.868		0.569		0.005	2.34	0.116		9,21,36,43,45,51
230494_at	Transcribed locus	SLC20A1	—	0.000	−2.45	0.909		0.008	−1.53	0.011		0.024		0.653		
227176_at	Solute carrier family 2, member 13	SLC2A13	Chr12q12	0.035		0.605		0.465		0.683		0.004	−2.37	0.027		56
235763_at	Solute carrier family 44, member 5	SLC44A5	Chr1p31.1	0.009	−4.13	0.351		0.276		0.158		0.025		0.639		—
225516_at	Solute carrier family 7, member 2	SLC7A2	Chr8p22-p21.3	0.001	4.91	0.740		0.012		0.045		0.191		0.478		18,42,43,45,46
239238_at	SWI/SNF related, subfamily c, member 1	SMARCC1	Chr3p23-p21	0.007	−2.06	0.340		0.285		0.218		0.013		0.442		—
201563_at	Sorbitol dehydrogenase	SORD	Chr15q15.3	0.117		0.007	−2.10	0.404		0.026		0.039		0.973		33,44
201418_s_at	SRY (sex determining region Y)-box 4	SOX4	Chr6p22.3	0.005	−2.21	0.999		0.048		0.135		0.112		0.881		1,3
213668_s_at	SRY (sex determining region Y)-box 4	SOX4	Chr6p22.4	0.004	−3.52	0.735		0.030		0.285		0.086		0.855		1,4
203017_s_at	Synovial sarcoma, X breakpoint 2 interacting protein	SSX2IP	Chr1p22.3	0.879		0.009	−2.10	0.097		0.041		0.446		0.526		12
202761_s_at	Spectrin repeat containing, nuclear envelope 2	SYNE2	Chr14q23.2	0.004	−3.94	0.511		0.139		0.125		0.029		0.773		3,8,14,15,31
232914_s_at	Synaptotagmin-like 2	SYTL2	Chr11q14	0.005	2.27	0.517		0.134		0.076		0.063		0.923		46
204158_s_at	T-cell, immune regulator 1, ATPase, isoform 3	TCIRG1	Chr11q13.2	0.007	−2.10	0.195		0.297		0.010	−2.04	0.161		0.358		37,48
206286_s_at	Teratocarcinoma-derived growth factor 1	TDGF1	Chr3p21.31	0.000	−3.84	0.056		0.140		0.000	−5.32	0.422		0.013		2,12,24
209651_at	Transforming growth factor beta 1 induced transcript 1	TGFB1I1	Chr16p11.2	0.005	−3.26	0.722		0.086		0.082		0.108		0.787		1,3,4,7,8,12
226319_s_at	THO complex 4	THOC4	Chr17q25.3	0.561		0.003	−2.57	0.012		0.158		0.247		0.875		19,20
224560_at	TIMP metallopeptidase inhibitor 2	TIMP2	Chr17q25	0.077		0.017		0.561		0.131		0.009	2.23	0.371		30
206271_at	Toll-like receptor 3	TLR3	Chr4q35	0.009	1.91	0.907		0.142		0.679		0.003	−2.05	0.043		9,14,27,28
219569_s_at	Transmembrane protein 22	TMEM22	Chr3q22.3	0.009	2.10	0.426		0.198		0.055		0.110		0.727		—
227062_at	Trophoblast-derived non-coding RNA	TncRNA	Chr11q13.1	0.014		0.128		0.636		0.241		0.005	3.08	0.269		—
234989_at	Trophoblast-derived non-coding RNA	TncRNA	Chr11q13.1	0.005	−2.48	0.169		0.353		0.078		0.011		0.645		—
228737_at	TOX high mobility group box family member 2	TOX2	Chr20q13.12	0.007	−2.44	0.505		0.018		0.276		0.229		0.850		3
220167_s_at	TP53TG3 protein	TP53TG3	Chr16p13	0.004	−2.64	0.931		0.043		0.020		0.435		0.216		—
219324_at	TRIO and F-actin binding protein/nucleolar protein 12	TRIOBP/ NOL12	Chr22q13.1	0.339		0.000	−2.11	0.024		0.004	1.59	0.006	−1.53	0.830		37
244610_x_at	Ubiquitin-conjugating enzyme E2E 2 (UBC4/5 homolog, yeast)	UBE2E2	Chr3p24.2	0.034		0.141		0.786		0.343		0.009	2.10	0.241		

218533_s_at	Uridine-cytidine kinase 1-like 1	UCKL1	Chr20q13.33	0.009	−2.30	0.682		0.110		0.061		0.192		0.577		16,32
212980_at	Ubiquitin-specific peptidase 34	USP34	Chr2p15	0.028		0.120		0.780		0.266		0.009	2.50	0.291		29
226176_s_at	Ubiquitin-specific peptidase 42	USP42	Chr7p22.1	0.006	−2.05	0.625		0.100		0.027		0.253		0.371		29
227894_at	WD repeat domain 90	WDR90	Chr16p13.3	0.000	−2.56	0.937		0.014		0.006	−1.92	0.166		0.273		
232389_at	WAS/WASL interacting protein family, member 3	WIPF3	—	0.000	−2.22	0.401		0.001	−1.62	0.007	−1.66	0.364		0.169		37,58
205990_s_at	Wingless-type MMTV integration site family, member 5A	WNT5A	Chr3p21-p14	0.001	4.71	0.580		0.012		0.435		0.013		0.435		1,14,24
205883_at	Zinc finger and BTB domain containing 16	ZBTB16	Chr11q23.1	0.005	−2.57	0.802		0.096		0.287		0.030		0.572		3,17,29
205383_s_at	Zinc finger and BTB domain containing 20	ZBTB20	Chr3q13.2	0.000	−2.11	0.550		0.055		0.078		0.006	1.69	0.653		3
235847_at	Zinc finger, AN1-type domain 3	ZFAND3	Chr6pter-p22.3	0.039		0.082		0.986		0.364		0.005	2.31	0.170		
206240_s_at	Zinc finger protein 136 (clone pHZ-20)	ZNF136	Chr19p13.2-12	0.004	−2.22	0.759		0.072		0.077		0.104		0.775		3,4
229765_at	Transcribed locus	ZNF207	—	0.507		0.008	2.16	0.147		0.078		0.104		0.908		3
219379_x_at	Zinc finger protein 358	ZNF358	Chr19p13.2	0.008	−2.04	0.948		0.066		0.123		0.168		0.756		3
55872_at	Zinc finger protein 512B	ZNF512B	Chr20q13.33	0.002	−2.20	0.189		0.175		0.004	−2.04	0.099		0.323		3
220617_s_at	Zinc finger protein 532	ZNF532	Chr18q21.32	0.001	−2.11	0.564		0.006	−1.55	0.023		0.376		0.250		3
229019_at	Zinc finger protein 533	ZNF533	Chr2q31.2-q31.3	0.010	−2.49	0.427		0.200		0.055		0.115		0.714		—
210679_x_at	Transcribed locus	—	—	0.006	−1.74	0.024		0.890		0.136		0.001	2.01	0.173		
215204_at	Transcribed locus	—	—	0.006	−2.49	0.717		0.032		0.278		0.117		0.937		
217679_x_at	Neuronal thread protein AD7c-NTP (*Homo sapiens*)	—	—	0.002	−2.03	0.076		0.501		0.163		0.001	2.18	0.182		
225239_at	Transcribed locus	—	—	0.003	−2.57	0.083		0.430		0.041		0.006	2.29	0.655		
226192_at	Predicted: similar to p40 (*H. sapiens*)	—	—	0.006	−2.36	0.282		0.006	−1.78	0.244		0.423		0.595		
227576_at	cDNA DKFZp686K1098	—	—	0.048		0.076		0.956		0.341		0.006	2.03	0.196		
227762_at	Transcribed locus	—	—	0.003	−2.08	0.122		0.492		0.315		0.001	2.35	0.116		
228854_at	Transcribed locus	—	—	0.006	−2.39	0.018		0.882		0.042		0.002	2.62	0.447		
229849_at	Predicted: similar to CR16 (Pan troglodytes)	—	—	0.004	−2.48	0.837		0.033		0.188		0.100		0.987		3
232156_at	Transcribed locus	—	—	0.001	2.11	0.514		0.014		0.508		0.026		0.484		
232397_at	*Homo sapiens*, clone IMAGE:4332461, mRNA	—	—	0.015		0.049		0.004	2.27	0.543		0.213		0.436		
232890_at	Neuronal thread protein AD7c-NTP	—	—	0.040		0.003	2.18	0.467		0.012		0.010		0.861		—
235028_at	Transcribed locus	—	—	0.006	−4.02	0.271		0.245		0.039		0.055		0.834		—
236934_at	Transcribed locus	—	—	0.901		0.037		0.088		0.346		0.005	2.02	0.007	−1.66	—
237154_at	Transcribed locus	—	—	0.002	2.09	0.022		0.646		0.013		0.003	−1.97	0.768		—
238717_at	CDNA FLJ31114 fis, clone IMR322000379	—	—	0.287		0.059		0.405		0.915		0.004	−2.74	0.027		—
239587_at	Transcribed locus	—	—	0.018		0.305		0.518		0.718		0.003	−2.14	0.084		—
239798_at	Transcribed locus	—	—	0.094		0.034		0.005	2.05	0.793		0.472		0.345		—
241600_at	Similar to CR16 (Pan troglodytes)	—	—	0.007	−2.27	0.433		0.191		0.085		0.061		0.979		—
242080_at	Hypothetical protein KIAA0563	—	—	0.003	−2.17	0.322		0.208		0.136		0.009	1.91	0.517		—
242405_at	Transcribed locus	—	—	0.209		0.085		0.568		0.880		0.007	2.14	0.059		—
242907_at	Similar to unactive progesterone receptor, 23 kDa isoform 4	—	chr1p22.2	0.004	2.98	0.123		0.002	2.25	0.353		0.498		0.622		—
243907_at	Transcribed locus	—	—	0.008	−2.03	0.741		0.092		0.062		0.196		0.572		—
244661_at	EST, multiple location, contains repetitive sequences	—	—	0.248		0.126		0.571		0.567		0.003	−2.21	0.010	1.62	—

Gene annotation codes	
1	Wnt-signaling pathway
2	MAPK-signaling pathway
3	Regulation of transcription
4	Regulation of transcription from RNA polymerase II promoter
5	Cell cycle/G1_to_S_cell_cycle/regulation of mitosis
6	Protein kinase activity, protein amino acid phosphorylation
7	TGF_β receptor-signaling pathway
8	Androgen receptor-signaling pathway/estrogen receptor-signaling pathway/steroid hormone receptor activity
9	NF-κB cascade, JNK cascade
10	G-protein-coupled receptor
11	Notch-signaling pathway, BMP-signaling pathway
12	Cell adhesion, cell migration
13	Interleukin-6 receptor pathway
14	Signal transduction
15	Chemotaxis/cell–cell signaling
16	ATP binding/nucleotide binding
17	Apoptosis
18	Insulin receptor-signaling pathway
19	RNA binding, processing, splicing
20	mRNA processing, RNA transport
21	Response to unfolded protein
22	Protein complex assembly
23	Ribosome biogenesis and assembly
24	Development/male gonad development
25	Angiogenesis
26	Antigen processing and presentation of endogenous peptide antigen via MHC class I
27	Immune response/Complement_Activation_Classical pathway
28	Inflammatory response
29	Ubiquitin cycle
30	Extracellular matrix structural constituent/Matrix_Metalloproteinases
31	Known Ovarian_Infertility_Genes
32	Carbohydrate metabolic process
33	Glucose metabolism
34	Steroid biosynthetic process
35	Cholesterol metabolic process/lipid metabolic process/lipid and lipoprotein metabolism/glycerophospholipid metabolism
36	Energy reserve/metabolic process
37	Actin cytoskeleton organization and biogenesis
38	Pyridine nucleotide biosynthetic process/purine metabolism/nucleotide metabolic process
39	Response to estrogen stimulus
40	Establishment and/or maintenance of chromatin architecture
41	Telomere maintenance
42	Regulated by insulin
43	Glucose intolerance/insulin resistance
44	Response to hormone stimulus
45	Obesity/body weight
46	Organ morphogenesis/fat cell differentiation
47	Protein transport

Continued

Continued

Gene annotation codes	
48	Ion transport
49	Calcium ion binding
50	ER-nuclear-signaling pathway
51	Regulation of hormone secretion
52	Chondroitin sulfate biosynthetic process
53	Heat shock protein binding
54	Glycosaminoglycan biosynthetic process
55	Translation
56	Transmembrane transporter/carbohydrate transport
57	Mitochondrial ribosomal protein
58	Spermatogenesis
59	Histone mRNA 3′-end processing

For each of the probe set ID, the columns detail the gene symbol, the full gene name and the chromosomal location. The numerical value represents the fold change of the probe set that was differentially expressed in that comparison. The genes are presented in their alphabetical order. Due to redundancy of the oligonucleotide probes on the chips, in several cases, the same gene is represented by more than one probe set. Where a gene is present in more than one list, its FC value is presented several times.

Submitted on October 6, 2008; resubmitted on December 6, 2008; accepted on December 19, 2008